Temperature dependence of strains and stresses in undercritical cubic superlattices and heterojunctions

T. D. Wen and E. Anastassakis
Department of Physics, National Technical University, Zografou 157 80 Athens, Greece
(Received 28 December 1994; revised manuscript received 12 September 1995)

Strained superlattices and heterojunctions subject to variable temperature exhibit changes in their elastic and/or thermal strain and stress components, relative to their values at room temperature. We consider systems grown in arbitrary directions, with thicknesses smaller than the critical value (undercritical systems). In lowest order, the changes are linear with the temperature. The dependence on temperature of the thermal expansion coefficients is taken into account and shown to improve agreement with data. Criteria are established for predicting the form of such changes in any combination of material constituents. Specific applications are treated in detail and comparison is made with existing data from the literature. The effective linear thermal expansion coefficients of the structure, parallel and perpendicular to the direction of growth, are formulated explicitly. The present results are transcribed to the parallel problem of a hydrostatic pressure in the most general case; this extends previously published work, which refers to material constituents with a lattice misfit smaller than the bulk modulus misfit. The latter assumption is valid for most material combinations but not all.

I. INTRODUCTION

Strained superlattices (SL's) and heterojunctions (HJ's) have been studied extensively in recent years under various external conditions, a chief example being the tuning of strains by a hydrostatic pressure.[1–4] In this work we treat the temperature dependence of strains and stresses in SL's and HJ's grown along an arbitrary direction. Only terms linear in the temperature T are considered. Most, if not all, physical properties of crystals exhibit T dependence, especially when a phase transition is approached. In view of such physical possibilities, the full treatment of the problem is rather complicated and one can only approach it under certain simplifying assumptions that allow the major macroscopic temperature effects to be followed. In this context we assume, throughout the present paper, that no phase transitions occur in the temperature range considered, and that the thermal expansion law and Hooke's law are valid, i.e.,

$$a(T)=a(1+\beta\Delta T), \tag{1a}$$

$$\sigma_i=C_{ij}\varepsilon_j . \tag{1b}$$

β is the linear thermal expansion coefficient (TEC) and C_{ij} are the components, in suppressed index notation, of the elastic stiffness tensor. The latter are treated as independent of T. We define as $\Delta T=T-T_0$ any temperature interval relative to an arbitrary reference value T_0 (e.g., room temperature). The lattice constant of the cubic crystal at T_0 is denoted by a, while σ_i and ε_j are, respectively, the stress and strain tensor components. Their T dependence is the main subject of this investigation. In what follows, T_0 will not be shown explicitly as a functional variable, namely, we set $a(T_0)\equiv a$; the same applies for any other parameter.

The entire analysis is based on the presence of isotropic in-plane strains, which appear after growth in the layers of HJ's and SL's and are due to mismatch of the constituents' lattice constants (*misfit strains*) and/or differences in their thermal expansion coefficients (*thermal strains*). Whether one or the other type of strain occurs in a particular system depends on the thickness h of the system, in relation to its critical thickness h_c. The latter determines an upper limit for coherent growth of the system.[5] In *undercritical* systems, which we consider here (i.e., $h\leqslant h_c$), the strains are uniform over the entire volume of the layer and do not normally depend on the growth temperature T_g. In *overcritical* systems ($h>h_c$) the strains are of mixed type, *misfit and thermal*, they depend on T_g and h and are not uniform over the layer's volume. In excessively thick systems the strains are purely thermal. Overcritical systems are more complicated in this regard and will be studied in a future work.

In the work of Ref. 2, referred to as EA from now on, the general criteria were established for predicting the behavior under P of any strained *undercritical* SL or HJ grown along an arbitrary direction. The entire analysis was based on the assumption that the lattice misfit $f=(a_2/a_1)-1$ (percentage difference of the lattice parameters of the two material constituents) was smaller than the misfit of the corresponding bulk moduli $\Delta B/B_1$, where $\Delta B=B_2-B_1$. The latter assumption is valid for most material combinations known and was not stated explicitly in EA. Through the present results it is possible to extend the work of EA on P effects to those cases not covered therein. A close look into the P and T effects allows one to transcribe the corresponding relations between the two types of effects through the following substitutions,

$$P\rightarrow-\Delta T,\quad B_\nu\rightarrow 1/3\beta_\nu,\quad \Delta B\rightarrow-\delta\beta/3\beta_1\beta_2, \tag{2}$$

where $\Delta\beta=\beta_2-\beta_1$. It should be remembered that P stands for the absolute value of the pressure (>0) whereas $\Delta T=T-T_0$ can take negative as well as positive values. In view of these facts, those P results not appearing in EA will be derived by use of (2) and inserted in the text following the corresponding T results.

This paper is based on certain results that have appeared in previous publications and will not be repeated here. These are: (i) A compact method for transforming fourth-rank tensor properties of cubic crystals from the system of crystallographic axes x_1, x_2, x_3, to any other system of orthogonal axes x_1', x_2', x_3' (Ref. 6). (ii) A detailed analysis of strains and stresses, in undercritical cubic SL's and HJ's, which are grown along an arbitrary direction.[7–9] (iii) Tuning of such strains and stresses by use of pressure.[2] In what follows, all primed (unprimed) quantities refer to the primed (unprimed) system. The direction cosines of x_λ' relative to x_1, x_2, x_3 are designated by $l_\lambda, m_\lambda, n_\lambda$, $\lambda=1,2,3$, and are considered to be known. The direction of growth is along $\mathbf{N} \| x_3'$. The two material constituents in SL's are designated by the material indices ν and ν', where $\nu'=2,1$ when $\nu=1,2$, respectively. For HJ's, the epilayer ($\nu=1$) takes the index e, or no index at all, and the substrate ($\nu=2$) takes the index s. More background information is included in the Appendix.

II. STRAINS IN UNDERCRITICAL SYSTEMS ($h \leqslant h_c$)

The physical origin of the misfit strains in undercritical systems is the mismatch between the lattice parameters of the two materials involved. It is convenient to define the lattice mismatch in a more symmetrical way than usually found in the literature, i.e., $f_\nu=(a_2-a_1)/a_\nu$. We examine HJ's and SL's separately.

A. Heterojunctions

At the growth temperature (T_g) the layer grows on the substrate coherently and remains in registry with it, parallel to the plane, at all temperatures thereafter. The expansion or contraction of the layer along any direction within the plane *is driven by the isotropic linear TEC of the substrate* β_s. The resulting in-plane elastic strain in the layer is

$$\varepsilon^{\|}(T,T)=a_s(T)/a(T)-1, \tag{3a}$$

where $a_s(T)$ and $a(T)$ stand for the lattice constants of the substrate and the layer at *any* temperature T. It should be noted that (3a) defines the strain $\varepsilon^{\|}$ of the layer at any temperature T, in terms of the layer's lattice constant at the same temperature T. This is the meaning of the double appearance of T on the left-hand side of (3a). In this work we define the strains relative to the lattice constant at T_0, i.e.,

$$\varepsilon^{\|}(T,T_0)=a_s(T)/a(T_0)-1=a_s(T)/a-1. \tag{3b}$$

It is easy to show that

$$\varepsilon^{\|}(T,T) \simeq \varepsilon^{\|}(T,T_0)-\beta\Delta T. \tag{3c}$$

At $T=T_0$ the two definitions coincide, as expected. Instead of β, the TEC of the layer, it is more appropriate to use the mean value of β in the region $\Delta T=T-T_0$, i.e.,

$$\bar{\beta}\Delta T=\int_{T_0}^{T}\beta(T)dT. \tag{4}$$

Usually in the literature the distinction between β and $\bar{\beta}$ is overlooked. It will be shown in Sec. V that handling the TEC properly, i.e., using $\bar{\beta}$ instead of β, improves the agreement between theory and experiment.

The remaining strain and stress components are related to $\varepsilon^{\|}$ through elasticity theory (Appendix). Equations (3) hold for any direction of growth of the HJ and not just for growth along [001] (Ref. 8). It is emphasized that the in-plane values of the linear TEC, $\beta^{\|}$, and the lattice constant, $a^{\|}$, of the layer coincide with those of the substrate, β_s, and a_s, respectively. In short, we can write for all temperatures

$$a^{\|}(T)=a_s(T), \tag{5a}$$

$$\beta^{\|}(T)=\beta_s(T). \tag{5b}$$

The substrate itself remains cubic (isotropic) at all temperatures. The normal-to-the-plane lattice constant $a^{\perp}(T)$ of the layer is determined by elasticity theory[8] and so is its normal-to-the-plane TEC, $\beta^{\perp}(T)$.

B. Superlattices

The alternating layers of a SL have thicknesses h_ν and lattice constants a_ν. At T_g the two layers grow on each other coherently; at any other temperature T they remain in registry with each other, parallel to the plane, following a common in-plane lattice constant $a^{\|}(T)$, which is determined on thermodynamical grounds and depends on the direction of growth.[9] This generates an in-plane isotropic elastic strain on each layer that depends on $a^{\|}(T)$ and can be computed after $a^{\|}(T)$ is known. The connecting relations at T_0 are[9]

$$a^{\|}=\frac{h_1G_1a_1+h_2G_2a_2}{h_1G_1+h_2G_2}, \tag{6}$$

$$\varepsilon_\nu^{\|}=a^{\|}/a_\nu-1, \tag{7}$$

where G_ν are shear moduli (Appendix). The value $a^{\|}(T)$ at $T \neq T_0$ is given by an expression similar to (6), with all parameters substituted by their corresponding values at T (see Sec. III). The counterpart of (3a) and (3b) at any T become

$$\varepsilon_\nu^{\|}(T,T)=a^{\|}(T)/a_\nu(T)-1, \tag{8a}$$

$$\varepsilon_\nu^{\|}(T,T_0)=a^{\|}(T)/a_\nu-1=\varepsilon_\nu^{\|}(T,T)+\beta_\nu\Delta T. \tag{8b}$$

Once again, instead of β_ν it is more appropriate to use the mean value $\bar{\beta}_\nu$ defined by an expression analogous to (4).

The following SL parameters are defined and will be derived in the following section: (i) The in-plane linear thermal expansion coefficient $\beta_{\mathrm{SL}}^{\|}$ for the SL as a whole, (ii) the normal-to-the-plane expansion coefficient $\beta_\nu^{\perp}$ for either layer, (iii) a normal-to-the-plane expansion coefficient of the entire system $\beta_{\mathrm{SL}}^{\perp}$, (iv) the volume thermal expansion coefficient β_{SL} for the system as a whole. Analogous definitions hold for the compressibilities $\kappa_{\mathrm{SL}}^{\|}$, $\kappa_\nu^{\perp}$, $\kappa_{\mathrm{SL}}^{\perp}$, K_{SL}, and the bulk modulus β_{SL}, respectively.

III. GENERAL TREATMENT OF TEMPERATURE EFFECTS

In this section we establish the linear relations between the strain and stress components at T and those at T_0. Given that $\varepsilon_\nu^{\|}(T,T_0)$ and $\varepsilon_\nu^{\|}(T,T)$ are simply connected (Sec. II), we restrict the discussion to $\varepsilon_\nu^{\|}(T,T_0)$ and drop the parameter T_0. Superlattices are treated first; the results for HJ's will be given at the end of the section.

If the temperature changes from T_0 to $T=T_0+\Delta T$, the lattice constants and the thicknesses will be modified. Then, from (6) we find $a^{\parallel}(T)$

$$a^{\parallel}(T)=\frac{h_1(T)G_1a_1(T)+h_2(T)G_2a_2(T)}{h_1(T)G_1+h_2(T)G_2}$$

$$\simeq\frac{h_1G_1a_1(1+\beta_1\Delta T)+h_2G_2a_2(1+\beta_2\Delta T)}{h_1G_1+h_2G_2}$$

$$=a^{\parallel}+\frac{h_1G_1a_1\beta_1+h_2G_2a_2\beta_2}{h_1G_1+h_2G_2}\,\Delta T, \tag{9}$$

where we keep terms only to the lowest order of ΔT. Equation (9) is analogous to the one for the pressure-dependent in-plane lattice constant developed in Ref. 2. The expression for the in-plane isotropic strain $\varepsilon_\nu^{\parallel}(T)$ is obtained from (7), (8), and (9),

$$\varepsilon_\nu^{\parallel}(T)=\frac{a^{\parallel}(T)}{a_\nu}-1=\varepsilon_\nu^{\parallel}+[\beta_\nu+(-1)^{\nu'}\alpha_\nu^{\parallel}(\delta\beta+\beta_{\nu'}f_\nu)]\Delta T \tag{10a}$$

$$=\varepsilon_\nu^{\parallel}[1+(\delta\beta+\beta_{\nu'}f_\nu)\Delta T/f_\nu]+\beta_\nu\Delta T \tag{10b}$$

$$=\varepsilon_\nu^{\parallel}\left(1-\frac{\Delta T}{\Delta T_m}\right)+\beta_\nu\Delta T, \tag{10c}$$

where

$$\Delta T_m=T_m-T_0=-\frac{f_\nu}{\delta\beta+\beta_{\nu'}f_\nu}. \tag{11}$$

The *critical temperature* T_m introduced in (11) is actually independent of ν and will be discussed later. The numerical parameter $\alpha_\nu^{\parallel}$ is defined as

$$\alpha_\nu^{\parallel}=(-1)^{\nu'}\varepsilon_\nu^{\parallel}/f_\nu=\frac{h_{\nu'}G_{\nu'}}{h_1G_1+h_2G_2}<1, \tag{12a}$$

with $\alpha_1^{\parallel}+\alpha_2^{\parallel}=1$. The parameter $\alpha_\nu^{\perp}$ will be used shortly and is defined as

$$\alpha_\nu^{\perp}=(-1)^{\nu}\varepsilon_\nu^{\perp}/f_\nu=\alpha_\nu^{\parallel}(\Delta\tilde{\varepsilon}_\nu-1)>0. \tag{12b}$$

It is recalled that $\varepsilon_\nu^{\parallel}$ etc. correspond to T_0. The expressions in the brackets of (10b) and (10c) represent the conversion factor, which transforms the strain and stress components at T_0 to their counterparts at $T\neq T_0$, not including $\beta_\nu\Delta T$, the isotropic contribution. Accordingly, the tetragonal distortion at T is written as

$$\Delta\varepsilon_\nu(T)=\Delta\varepsilon_\nu[1+(\delta\beta+\beta_{\nu'}f_\nu)\Delta T/f_\nu] \tag{13a}$$

$$=\Delta\varepsilon_\nu\left(1-\frac{\Delta T}{\Delta T_m}\right), \tag{13b}$$

where $\Delta\varepsilon_\nu=\varepsilon_\nu^{\parallel}-\varepsilon_\nu^{\perp}$ is the tetragonal distortion at T_0 (see Appendix and Refs. 7 to 10 for explicit forms in various directions of growth). Furthermore, the normal-to-the-plane strains are

$$\varepsilon_\nu^{\perp}(T)=\varepsilon_\nu^{\parallel}(T)-\Delta\varepsilon_\nu(T)$$

$$=\varepsilon_\nu^{\perp}+[\beta_\nu+(-1)^{\nu}\alpha_\nu^{\perp}(\delta\beta+\beta_{\nu'}f_\nu)]\Delta T \tag{14a}$$

$$=\varepsilon_\nu^{\perp}[1+(\delta\beta+\beta_{\nu'}f_\nu)\Delta T/f_\nu]+\beta_\nu\Delta T \tag{14b}$$

$$=\varepsilon_\nu^{\perp}\left(1-\frac{\Delta T}{\Delta T_m}\right)+\beta_\nu\Delta T. \tag{14c}$$

The shear strains and all nonzero stress components at T are related to their counterparts at T_0 in the same way as (13) indicates, i.e.,

$$\varepsilon'_{\nu,4}(T)=\varepsilon'_{\nu,4}\left(1-\frac{\Delta T}{\Delta T_m}\right), \tag{15a}$$

$$\sigma'_{\nu,6}(T)=\sigma'_{\nu,6}\left(1-\frac{\Delta T}{\Delta T_m}\right), \tag{15b}$$

and likewise for $\varepsilon'_{\nu,5}(T),\sigma'_{\nu,1}(T),\sigma'_{\nu,2}(T)$.

The physical meaning of the critical temperature is that at T_m the tetragonal distortion of both layers becomes zero. Indeed, setting the expression in brackets of (13a) equal to zero yields the definition of (11). At this temperature $\varepsilon_\nu^{\perp}(T_m)$ equals $\varepsilon_\nu^{\parallel}(T_m)$, and both unit cells recover their cubic shape. The critical temperature exists for all material combinations, in principle. According to (11), it can be lower or higher than T_0, but in all cases it must be positive ($T_m>0$). If, for a particular material combination, Eq. (11) yields $T_m<0$, this means that there is no real temperature at which the unit cells of these materials, combined in an undercritical SL, recover their cubic shape. Such situations will be discussed in Sec. IV C. Notice, in Eqs. (10c), (14c), the separation of the isotropic strain contribution $\beta_\nu\Delta T$, due to volume thermal expansion, from the anisotropic part. The isotropic part is the only contribution to the strains at $T=T_m$.

The same results can be obtained independently from the generalized Hooke's law at any temperature T, written in the primed system in the following form[11]

$$\sigma'_i(T)=C'_{ij}[\varepsilon'_j(T)-\beta'_j\Delta T],\quad i,j=1-6, \tag{16}$$

where the layer index is dropped for simplicity. In cubic crystals β'_j is isotropic, i.e., $\beta'_j\equiv\beta$, and (16) takes the following form

$$\sigma'_i(T)=C'_{ij}\begin{cases}\varepsilon'_j(T)-\beta\Delta T, & j=1-3\\ \varepsilon'_j(T), & j=4-6.\end{cases} \tag{17}$$

Combining (17) with the conditions $\varepsilon'_1(T)=\varepsilon'_2(T)\equiv\varepsilon^{\parallel}(T)$; $\varepsilon'_3(T)\equiv\varepsilon_\nu^{\perp}(T);\varepsilon'_6(T)=0,\sigma'_3(T)=\sigma'_4(T)=\sigma'_5(T)=0$, yields the same results obtained above by using the conversion factor of (10b) or (10c).

Next we derive the linear TEC's of the layers, for directions parallel and perpendicular to the direction of growth. Such information may be particularly useful in analyzing experimental data of x-ray diffraction under variable temperature.

Because of the coherent growth and the fact that $\beta_1\neq\beta_2$, in general, the TEC of the structure, as a whole, is aniso-

tropic. To the lowest order of ΔT, the in-plane and normal-to-the-plane lattice constants are

$$a^{\parallel}(T)=a^{\parallel}(1+\beta_{\mathrm{SL}}^{\parallel}\Delta T), \tag{18a}$$

$$a_{\nu}^{\perp}(T)=a_{\nu}^{\perp}(1+\beta_{\nu}^{\perp}\Delta T). \tag{18b}$$

It is emphasized that $\beta_{\mathrm{SL}}^{\parallel}$ governs the in-plane TEC of the entire SL, whereas $\beta_{\nu}^{\perp}$ governs the TEC of each layer ν in the direction of growth. An expression for $\beta_{\mathrm{SL}}^{\parallel}$ can be obtained by combining (6), (9), and (18a),

$$\beta_{\mathrm{SL}}^{\parallel}\equiv\frac{1}{a^{\parallel}}\frac{da^{\parallel}(T)}{dT}=\frac{h_1G_1\beta_1a_1+h_2G_2\beta_2a_2}{h_1G_1a_1+h_2G_2a_2}. \tag{19}$$

For $\beta_{\nu}^{\perp}$ we use the definitions

$$\varepsilon_{\nu}^{\parallel}(T)=\frac{a^{\parallel}(T)}{a_{\nu}}-1,\quad \varepsilon_{\nu}^{\perp}(T)=\frac{a_{\nu}^{\perp}(T)}{a_{\nu}}-1, \tag{20}$$

which yield

$$a_{\nu}^{\perp}(T)=a^{\parallel}(T)-a_{\nu}\Delta\varepsilon_{\nu}(T), \tag{21a}$$

$$a_{\nu}^{\perp}=a^{\parallel}-a_{\nu}\Delta\varepsilon_{\nu}. \tag{21b}$$

Upon combining (18b), (20), and (21) we obtain, in lowest order,

$$\beta_{\nu}^{\perp}=\frac{1}{a_{\nu}^{\perp}}\frac{da_{\nu}^{\perp}(T)}{dT}\simeq\beta_{\mathrm{SL}}^{\parallel}-(\delta\beta+\beta_{\nu'}f_{\nu})\Delta\varepsilon_{\nu}/f_{\nu}. \tag{22}$$

The normal-to-the-plane TEC of the entire SL, considered as one entity, is easily shown to be

$$\beta_{\mathrm{SL}}^{\perp}=\frac{h_1\beta_1^{\perp}+h_2\beta_2^{\perp}}{h_1+h_2}. \tag{23}$$

The volume expansion coefficient of the entire SL is defined as

$$\beta_{\mathrm{SL}}=2\beta_{\mathrm{SL}}^{\parallel}+\beta_{\mathrm{SL}}^{\perp}. \tag{24}$$

The above results are easily adapted to HJ's. Here $f=a_s/a-1$, $\delta\beta=\beta_s-\beta$, $h_s\gg h$, and

$$\varepsilon^{\parallel}=f,\quad \varepsilon^{\perp}=f-\Delta\varepsilon,\quad \varepsilon_s^{\parallel}=\varepsilon_s^{\perp}=\Delta\varepsilon_s=0,\quad a^{\parallel}=a_s, \tag{25a}$$

$$\alpha^{\parallel}=1,\quad \alpha^{\perp}=\Delta\tilde{\varepsilon}-1,\quad \alpha_s^{\parallel}=\alpha_s^{\perp}=0, \tag{25b}$$

where $\Delta\varepsilon=f\Delta\tilde{\varepsilon}$. The expressions for $\Delta\tilde{\varepsilon}$ in various directions of growth are the same as for the corresponding SL's and can be found in Refs. 7–10. Explicit results for HJ's will be given in Sec. IV B.

Next, starting from (10), we write the corresponding expressions for the effects of a pressure $-P$ ($P>0$), following the substitutions (2), as discussed earlier. Now all linear dimensions of a cubic material contract by the factor $(1-P/3B)$ and it is assumed that the shear moduli G_{ν} are independent of P. The P-dependent in-plane strains *relative to the* $P=0$ *state* are

$$\varepsilon_{\nu}^{\parallel}(P)=\frac{a^{\parallel}(P)}{a_{\nu}}-1$$

$$=\varepsilon_{\nu}^{\parallel}-\frac{P}{3B_1B_2}[B_{\nu'}+(-1)^{\nu}\alpha_{\nu}^{\parallel}(\Delta B-f_{\nu}B_{\nu})] \tag{26a}$$

$$=\varepsilon_{\nu}^{\parallel}\left[1+\frac{P}{3B_1B_2f_{\nu}}(\Delta B-f_{\nu}B_{\nu})\right]-\frac{P}{3B_{\nu}} \tag{26b}$$

$$=\varepsilon_{\nu}^{\parallel}\left(1-\frac{P}{P_m}\right)-\frac{P}{3B_{\nu}}, \tag{26c}$$

where

$$P_m=\frac{3B_1B_2f_{\nu}}{f_{\nu}B_{\nu}-\Delta B}=\frac{f_{\nu}}{f_{\nu}\kappa_{\nu'}+\Delta\kappa}. \tag{27}$$

$\kappa_{\nu}=1/3B_{\nu}$ is the linear compressibility of layer ν and $\Delta\kappa=\kappa_2-\kappa_1$. The brackets in (26b) and (26c) are the conversion factors, which allow one to write

$$\Delta\varepsilon_{\nu}(P)=\Delta\varepsilon_{\nu}\left[1+\frac{P}{3B_1B_2f_{\nu}}(\Delta B-f_{\nu}B_{\nu})\right] \tag{28a}$$

$$=\Delta\varepsilon_{\nu}\left(1-\frac{P}{P_m}\right) \tag{28b}$$

$$=\left[\varepsilon_{\nu}^{\parallel}(P)+\frac{P}{3B_{\nu}}\right]\Delta\tilde{\varepsilon}_{\nu}. \tag{28c}$$

$$\varepsilon_{\nu}^{\perp}(P)=\varepsilon_{\nu}^{\parallel}(P)-\Delta\varepsilon_{\nu}(P)$$

$$=\varepsilon_{\nu}^{\perp}-\frac{P}{3B_1B_2}[B_{\nu'}+(-1)^{\nu'}\alpha_{\nu}^{\perp}(\Delta B-f_{\nu}B_{\nu})] \tag{29a}$$

$$=\varepsilon_{\nu}^{\perp}\left[1+\frac{P}{3B_1B_2f_{\nu}}(\Delta B-f_{\nu}B_{\nu})\right]-\frac{P}{3B_{\nu}} \tag{29b}$$

$$=\varepsilon_{\nu}^{\perp}\left(1-\frac{P}{P_m}\right)-\frac{P}{3B_{\nu}} \tag{29c}$$

$$=\varepsilon_{\nu}^{\parallel}(P)(1-\Delta\tilde{\varepsilon}_{\nu})-\frac{P}{3B_{\nu}}\Delta\tilde{\varepsilon}_{\nu}. \tag{29d}$$

Equations (26)–(29) differ from the corresponding ones in EA by the presence of the term $f_{\nu}B_{\nu}$, which can be neglected in the cases considered in EA. Mathematically, the pressure P_m can be positive, negative, or zero, according to the definition (27). When positive, P_m stands for the physically meaningful *critical pressure*, for which $\Delta\varepsilon_{\nu}(P_m)=0$. The requirement for $P_m>0$ is that $B_{\nu}f_{\nu}-\Delta B$ and f_{ν} have the same sign for either value of ν.

The compressibilities $\kappa_{\mathrm{SL}}^{\parallel}$, $\kappa_{\mathrm{SL}}^{\perp}$, K_{SL}, and the bulk modulus B_{SL} have the same forms as in EA; the compressibility $\kappa_{\nu}^{\perp}$ now takes the form

$$\kappa_\nu^\perp = -\frac{da_\nu^\perp(P)}{dP} \Big/ a_\nu^\perp = \kappa_{\rm SL}^\parallel + (f_\nu\kappa_\nu - \Delta\kappa)\Delta\varepsilon_\nu/f_\nu. \quad (30)$$

This differs from EA by the $f_\nu\kappa_\nu$ term, which can be neglected in the cases considered in EA. In the case of HJ's all the above results are valid with $h_2 \gg h_1$. Explicit results will be given in Sec. IV B.

IV. CLASSIFICATION OF UNDERCRITICAL STRUCTURES

The results in Sec. III can be further simplified depending on the relative magnitude of the two terms inside the parentheses in the right-hand side of (10), (11), (13), and (14) for T effects, or (26)–(29) for P effects. We consider the three possible cases separately.

A. $|f_\nu| \ll |\delta\beta/\beta_{\nu'}|$

Most material combinations satisfy the condition $|f_\nu| \ll |\delta\beta/\beta_{\nu'}|$, e.g., AlAs/GaAs, AlAs/Ge, AlAs/ZnS, AlAs/Si, GaAs/Ge, InSb/AlSb, InSb/CdTe, InSb/HgTe, ZnS/Si, ZnSe/Si, and AlP/GaP, GaAs/GaP, GaAs/InAs, GaAs/Si, GaP/Si, GaSb/AlSb, Ge/Si, InAs/GaSb, InAs/Si, ZnS/GaP, ZnSe/AlAs, ZnSe/GaAs, ZnSe/Ge, ZnTe/AlSb, ZnTe/GaSb, ZnTe/InAs.

The difference between f_1 and f_2 now can be ignored, i.e., we set $f_1 \equiv f$ and $f_2 \simeq f_1$. Equations (10)–(15) become

$$\varepsilon_\nu^\parallel(T) = \varepsilon_\nu^\parallel + (\beta_\nu + (-1)^{\nu'}\alpha_\nu^\parallel\delta\beta)\Delta T, \quad (31a)$$

$$\Delta\varepsilon_\nu(T) = \Delta\varepsilon_\nu(1 + \delta\beta\Delta T/f\ ), \quad (31b)$$

$$\varepsilon_\nu^\perp(T) = \varepsilon_\nu^\perp + [\beta_\nu + (-1)^\nu\alpha_\nu^\perp\delta\beta]\Delta T, \quad (31c)$$

$$\varepsilon'_{\nu,4}(T) = \varepsilon'_{\nu,4}(1 + \delta\beta\Delta T/f\ ), \quad (32a)$$

$$\sigma'_{\nu,6}(T) = \sigma'_{\nu,6}(1 + \delta\beta\Delta T/f\ ), \ \text{etc.}, \quad (32b)$$

$$\Delta T_m = T_m - T_0 = -\frac{f}{\delta\beta} = \frac{a_1 - a_2}{a_1(\beta_2 - \beta_1)}. \quad (33)$$

The linear trends of $\varepsilon_1^\parallel(T)$ and $\varepsilon_1^\perp(T)$ as a function of T are shown schematically in Fig. 1, with the strain axis placed at T_0. The following comments apply here: (i) The values $\varepsilon_1^\parallel$ and $\varepsilon_1^\perp$ at T_0 have opposite signs. (ii) The slopes of the curves for $\varepsilon_1^\parallel(T)$ are always positive, whereas those for $\varepsilon_1^\perp(T)$ can be positive, zero, or negative. (iii) The two lines always intercept at T_m, which may be higher than T_0 (when $f/\delta\beta < 0$), equal to T_0 ($f = 0$), or lower than T_0 ($f/\delta\beta > 0$); in the latter case, the condition for T_m to be physically meaningful, $T_m > 0$, is $f/\delta\beta < T_0$ and this is not always satisfied. If $f/\delta\beta \geq T_0$, the two lines never intercept and T_m is simply a mathematical parameter with no physical meaning. (iv) There is no row in the Fig. 1 with $\delta\beta = 0$ since such material combinations could not be consistent with the basic assumption of $|f_\nu| \ll |\delta\beta/\beta_{\nu'}|$. The functions $\varepsilon_2^\parallel(T)$, $\varepsilon_2^\perp(T)$ can be discussed in the same way.[2]

The TEC parallel to the plane introduced in (19) continues to hold, whereas (22)–(24) become

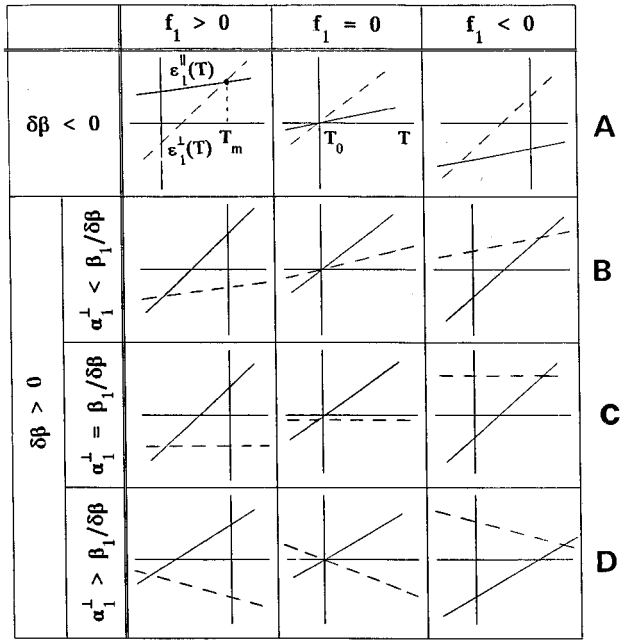

FIG. 1. Schematic presentation of the linear functions $\varepsilon_1^\parallel(T)$ and $\varepsilon_1^\perp(T)$ for material combinations satisfying the condition $|f_\nu| \ll |\delta\beta/\beta_{\nu'}|$. The critical temperature T_m can be higher than, lower than, or equal to T_0, the room temperature. For an HJ grown along [001] the condition or inequality in row B becomes $2C_{12}/C_{11} < \beta/\delta\beta$. Analogous changes apply to rows C and D, respectively. $\delta\beta$ stands for $\beta_2 - \beta_1$ or $\beta_s - \beta$.

$$\beta_\nu^\perp = \beta_{\rm SL}^\parallel - \Delta\varepsilon_\nu\frac{\delta\beta}{f_\nu} \quad (34a)$$

$$\beta_{\rm SL}^\perp = \frac{h_1\beta_1^\perp + h_2\beta_2^\perp}{h_1 + h_2} = \beta_{\rm SL}^\parallel - \frac{h_1\Delta\varepsilon_1/f_1 + h_2\Delta\varepsilon_2/f_2}{h_1 + h_2}\,\delta\beta, \quad (34b)$$

$$\beta_{\rm SL} = 2\beta_{\rm SL}^\parallel + \beta_{\rm SL}^\perp = 3\beta_{\rm SL}^\parallel - \frac{h_1\Delta\varepsilon_1/f_1 + h_2\Delta\varepsilon_2/f_2}{h_1 + h_2}\,\delta\beta. \quad (34c)$$

The above results combined with (25) yield for HJ's

$$\varepsilon^\parallel(T) = f + \beta_s\Delta T, \quad (35a)$$

$$\Delta\varepsilon(T) = \Delta\varepsilon[1 + \delta\beta\Delta T/f], \quad (35b)$$

$$\varepsilon^\perp(T) = \varepsilon^\perp + [\beta_s - \Delta\tilde{\varepsilon}\,\delta\beta]\Delta T. \quad (35c)$$

The substrates change isotropically, i.e., all strains are equal to $\beta_s\Delta T$. Thus

$$a^\parallel(T) = a_s^\parallel(T) = a_s^\perp(T) = a_s(T) = a_s(1 + \beta_s\Delta T). \quad (36a)$$

Furthermore, (18b) and (21a) give

$$a^\perp(T) = a^\perp(1 + \beta^\perp\Delta T) = a_s(T) - a\Delta\varepsilon(T). \quad (36b)$$

The TEC's for an HJ are obtained in a similar manner,

$$\beta_{\mathrm{HJ}}^{\parallel}=\beta_{\mathrm{HJ}}^{\perp}=\beta_s^{\perp}=\beta_s, \tag{37a}$$

$$\beta^{\perp}=\beta_s-\delta\beta\Delta\varepsilon/f, \tag{37b}$$

$$\beta_{\mathrm{HJ}}=3\beta_s. \tag{37c}$$

The corresponding situation for P effects arises when $|f_\nu|\ll|\Delta B/B_\nu|$. This is the case treated thoroughly in EA, with $f_1\equiv f$ and $f_2\simeq f_1$. Most material combinations belong to this case, e.g., the entire second group tabulated before Eq. (31a) and InAs/InP, InAs/AlSb, ZnS/ZnSe, GaP/InP. In this case the $f_\nu B_\nu$ term in $\Delta B-f_\nu B_\nu$ can be dropped and the results for SL's and HJ's are as in EA. Clearly, material combinations with $\Delta B=0$ cannot satisfy the condition $|f|\ll|\Delta B/B|$. Such are the cases included in row B of Fig. 1 and column B of Fig. 2 in EA; both should be ignored. The combination InP/GaAs appearing in the compilation after Eq. (28) of EA should also be ignored as belonging to the following subcategory. All other conclusions in EA remain valid.

B. $|f_\nu|\simeq|\delta\beta/\beta_{\nu'}|$

In this section we examine situations that satisfy the condition $|f_\nu|\simeq|\delta\beta/\beta_{\nu'}|$. Fewer but well-known combinations belong to this case, e.g., ZnSe/ZnTe, InAs/InP, ZnSe/ZnS, ZnS/GaAs.

Now, the general results of Sec. III are directly applicable without further simplifications. The linear trends of $\varepsilon_1^{\parallel}(T)$ and $\varepsilon_1^{\perp}(T)$ are shown in Fig. 2. There are now fifteen entries according to the sign combinations of f_1 and $f_1\beta_2+\delta\beta$. Otherwise, the same comments made after (33) continue to hold, except that now it is Eq. (11) that determines whether T_m is real and higher than, lower than, or equal to T_0.

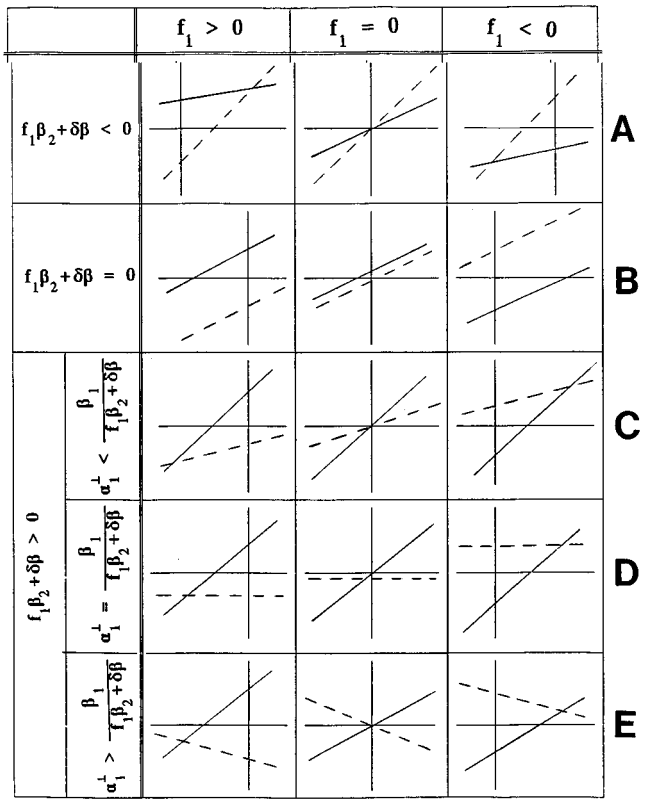

FIG. 2. Same as Fig. 1 under the condition $|f_\nu|\simeq|\delta\beta/\beta_{\nu'}|$. For HJ's along [001] the condition or inequality in row C becomes $2C_{12}/C_{11}<\beta/(\delta\beta+f\beta_s)$. Analogous changes apply to rows D and E, respectively.

For HJ's the results follow directly from Sec. III and (25)

$$\varepsilon^{\parallel}(T)=f+(1+f)\beta_s\Delta T, \tag{38a}$$

$$\Delta\varepsilon(T)=\Delta\varepsilon[1+(\delta\beta+f\beta_s)\Delta T/f] \tag{38b}$$

$$=[\varepsilon^{\parallel}(T)-\beta\Delta T]\Delta\tilde{\varepsilon}, \tag{38c}$$

$$\varepsilon^{\perp}(T)=\varepsilon^{\perp}+[\beta+(1-\Delta\tilde{\varepsilon})(\delta\beta+f\beta_s)]\Delta T \tag{38d}$$

$$=\varepsilon^{\parallel}(T)(1-\Delta\tilde{\varepsilon})+\beta\Delta T\Delta\tilde{\varepsilon}, \tag{38e}$$

$$\varepsilon_s^{\parallel}(T)=\varepsilon_s^{\perp}(T)=\beta_s\Delta T,\quad \Delta\varepsilon_s(T)=0, \tag{39}$$

$$\Delta T=-\frac{f}{\delta\beta+f\beta_s}, \tag{40}$$

$$\beta_{\mathrm{HJ}}^{\parallel}=\beta_{\mathrm{HJ}}^{\perp}=\beta_s^{\perp}=\beta_s, \tag{41a}$$

$$\beta_{\mathrm{HJ}}=3\beta_s, \tag{41b}$$

$$\beta^{\perp}=\beta_s-(\beta_s+\delta\beta/f)\Delta\varepsilon,\quad \delta\beta=\beta_s-\beta. \tag{41c}$$

The corresponding situation for P effects arises when $|f_\nu|\simeq|\Delta B/B_\nu|$. The general results of Sec. III are directly applicable without further simplifications. There are not so many material combinations belonging to this category, e.g., InP/GaAs, GaAs/Ge, ZnTe/InSb, AlSb/ZnSe. The functions $\varepsilon_\nu^{\parallel}(P)$ and $\varepsilon_\nu^{\perp}(P)$ given by (26) and (29) for layer 1 are shown schematically in Fig. 3. The slope of $\varepsilon_1^{\parallel}(P)$ is always negative. The slope of $\varepsilon_1^{\perp}(P)$ can be positive, zero, or negative. There are fifteen combinations for these slopes in pairs according to the signs of f_1 and $f_1B_1-\Delta B$. The pressure range in all cases is limited to $P\leqslant P_{\max}$, where $P_{\max}$ is the limit of linear effects; it is assumed, further, that no phase transitions occur in that range. There are four configurations where the two lines cross each other at $P_m(>0)$. These are the cases where f_1 and $f_1B_1-\Delta B$ have the same sign. The fifteen entries coincide one to one with those in Fig. 1 of EA, except that row B of the latter should be eliminated, as explained in Sec. IV A.

For HJ's the results follow directly from Sec. III and (25)

$$\varepsilon^{\parallel}(P)=f-\frac{P}{3B_s}(1+f), \tag{42a}$$

$$\Delta\varepsilon(P)=\Delta\varepsilon\left[1+\frac{P}{3BB_sf}(\Delta B-fB)\right] \tag{42b}$$

$$=\left[\varepsilon^{\parallel}(P)+\frac{P}{3B}\right]\Delta\tilde{\varepsilon}, \tag{42c}$$

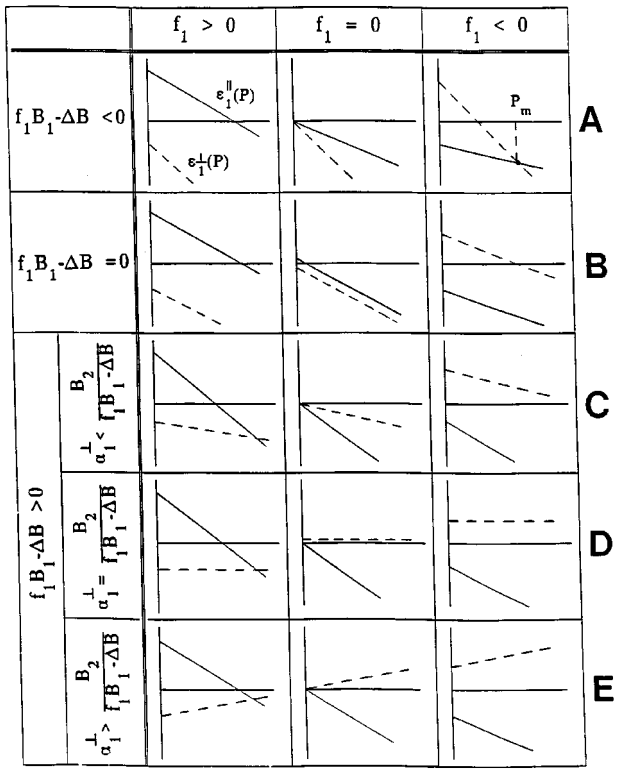

FIG. 3. Same as Fig. 1 as a function of P, under the condition $|f_\nu| \simeq |\Delta B/B_\nu|$. For HJ's along [001] the condition imposed by $\alpha_1^\perp$ in row C becomes $3B^s > 2C_{12}^e(1+f\,)$. Analogous changes apply to rows D and E.

$$\varepsilon^\perp(P) = \varepsilon^\perp - \frac{P}{3BB_s}\,[B_s + (\Delta\tilde{\varepsilon} - 1)(\Delta B - fB)] \quad (42d)$$

$$= \varepsilon^\parallel(P)(1 - \Delta\tilde{\varepsilon}) - \frac{P}{3B}\,\Delta\tilde{\varepsilon}, \quad (42e)$$

$$\varepsilon_s^\parallel(P) = \varepsilon_s^\perp(P) = -\frac{P}{3B_s}, \quad \Delta\varepsilon_s(P) = 0, \quad (43)$$

$$P_m = \frac{3BB_s f}{fB - \Delta B}, \quad (44)$$

$$\kappa_{\rm HS}^\parallel = \kappa_{\rm HS}^\perp = \kappa_s^\perp = \kappa_s\,, \quad (45a)$$

$$K_{\rm HS} = 3\kappa_s = 1/B_{\rm HS}\,, \quad (45b)$$

$$\kappa^\perp = \kappa_s + (f\kappa - \Delta\kappa)\Delta\varepsilon/f, \quad \Delta\kappa = \kappa_s - \kappa. \quad (45c)$$

C. $|f_\nu| \gg |\delta\beta/\beta_{\nu'}|$

This case is also rather rare, e.g., CdTe/GaP, ZnSe/GaSb, AlAs/CdTe, GaP/InP.

All expressions for the strain and stress components can be obtained by dropping the term $\delta\beta$ from Eqs. (10)–(14). The results are

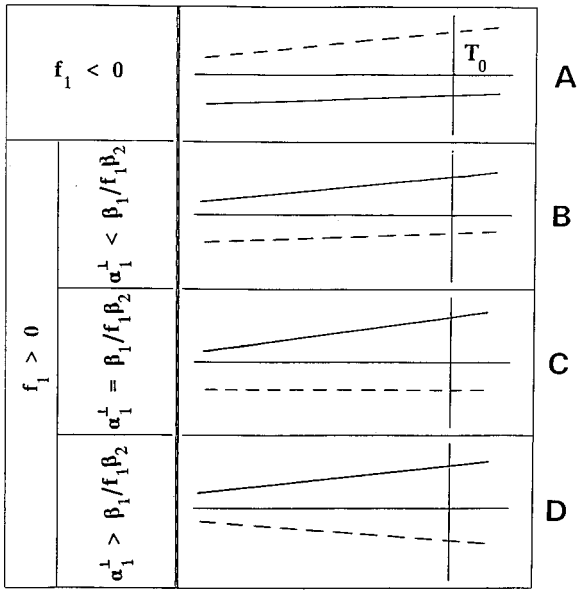

FIG. 4. Same as Fig. 1 under the condition $|f_\nu| \gg |\delta\beta/\beta_{\nu'}|$. For HJ's along [001] the condition or inequality in row B becomes $2C_{12}/C_{11} < \beta/f\beta_s$. Analogous changes apply to rows C and D, respectively.

$$\varepsilon_\nu^\parallel(T) = \varepsilon_\nu^\parallel + [\beta_\nu + (-1)^{\nu'}\alpha_\nu^\parallel\beta_{\nu'}f_\nu]\Delta T$$
$$= \varepsilon_\nu^\parallel(1 + \beta_{\nu'}\Delta T) + \beta_\nu\Delta T, \quad (46a)$$

$$\Delta\varepsilon_\nu^\parallel(T) = \Delta\varepsilon_\nu^\parallel(1 + \beta_{\nu'}\Delta T), \quad (46b)$$

$$\varepsilon_\nu^\perp(T) = \varepsilon_\nu^\perp + [\beta_\nu + (-1)^\nu\alpha_\nu^\perp\beta_{\nu'}f_\nu]\Delta T$$
$$= \varepsilon_\nu^\perp(1 + \beta_{\nu'}\Delta T) + \beta_\nu\Delta T. \quad (46c)$$

Equations (15) are valid with

$$\Delta T_m = -1/\beta_{\nu'}\,. \quad (47)$$

In this case T_m stands for a mathematical parameter with no physical meaning, since $T_m < 0$. Indeed, for all types of materials β varies from 10^{-6}/K to 10^{-5}/K, hence T_m is between -10^5 and -10^6 K. The expansion coefficients $\beta_{\rm SL}^\parallel$, $\beta_{\rm SL}^\perp$, $\beta_{\rm SL}$ are as in Sec. III, with

$$\beta_\nu^\perp = \beta_{\rm SL}^\parallel - \beta_{\nu'}\Delta\varepsilon_\nu\,. \quad (48)$$

Figure 4 shows schematically the linear trends of $\varepsilon_1^\parallel(T)$ and $\varepsilon_1^\perp(T)$. Notice the absence of the $f=0$ row, which cannot satisfy the condition $|f_\nu| \gg |\delta\beta/\beta_{\nu'}|$. Only four possibilities exist. In all cases the curves are practically parallel, since the ''critical temperatures'' now move to minus infinity.

For HJ's the results follow directly from (38)–(41) after dropping the term $\delta\beta$, or (46) and (47) together with (25):

$$\varepsilon^\parallel(T) = (\beta + \beta_s f\,)\Delta T, \quad (49a)$$

$$\Delta\varepsilon(T) = \Delta\varepsilon(1 + \beta_s\Delta T), \quad (49b)$$

$$\varepsilon^\perp(T) = \varepsilon^\perp + [\beta + (1 - \Delta\tilde{\varepsilon})f\beta_s]\Delta T, \quad (49c)$$

$$\varepsilon_s^\parallel(T) = \varepsilon_s^\perp(T) = \beta_s\Delta T, \quad \Delta\varepsilon_s(T) = 0, \quad (50)$$

$$\Delta T_m = -1/\beta_s . \tag{51}$$

The TEC's are as in Eqs. (41a) and (41b), and

$$\beta^{\perp} = \beta_s (1 - \Delta\varepsilon). \tag{52}$$

The corresponding situation for P effects arises when $|f_\nu| \gg |\Delta B/B_\nu|$. This case is also rather rare (AlSb/InAs, ZnS/GaAs). Here, the general results of Sec. III take the form

$$\varepsilon_\nu^{\parallel}(P) = \varepsilon_\nu^{\parallel} - \frac{P}{3B_1B_2}\left[B_{\nu'} + (-1)^{\nu'}\alpha_\nu^{\parallel} f_\nu B_\nu\right]$$

$$= \varepsilon_\nu^{\parallel}\left(1 - \frac{P}{3B_{\nu'}}\right) - \frac{P}{3B_\nu}, \tag{53a}$$

$$\Delta\varepsilon_\nu(P) = \Delta\varepsilon_\nu\left(1 - \frac{P}{3B_{\nu'}}\right), \tag{53b}$$

$$\varepsilon_\nu^{\perp}(P) = \varepsilon_\nu^{\perp} - \frac{P}{3B_1B_2}\left[B_{\nu'} + (-1)^{\nu}\alpha_\nu^{\perp} f_\nu B_\nu\right]$$

$$= \varepsilon_\nu^{\perp}\left(1 - \frac{P}{3B_{\nu'}}\right) - \frac{P}{3B_\nu}, \tag{53c}$$

$$P_m = \frac{3B_1B_2 f_\nu}{f_\nu B_\nu - \Delta B} \approx 3B_{\nu'} . \tag{54}$$

At first glance (54) seems to imply that the critical pressure P_m ($\approx 3B_{\nu'}$) is different for the two layers. This is a mathematical consequence of the approximation $|f| \gg |\Delta B/B|$. The exact formula for P_m yields for both layers the same value, which, in fact, is very close to $3B_{\nu'}$. An analogous comment holds for (47).

The linear compressibilities $\kappa_{\mathrm{SL}}^{\parallel}$, $\kappa_{\mathrm{SL}}^{\perp}$, K_{SL}, and the bulk modulus B_{SL} are as in Sec. II, while

$$\kappa_\nu^{\perp} = \kappa_{\mathrm{LS}}^{\parallel} + \kappa_\nu \Delta\varepsilon_\nu . \tag{55}$$

Figure 5 shows schematically the trends of $\varepsilon_1^{\parallel}(P)$ and $\varepsilon_1^{\perp}(P)$. A total of four possibilities exist. Notice the absence of the $f=0$ column, which cannot satisfy the condition $|f| \gg |\Delta B/B|$. The critical pressure P_m exists in principle for the four cases, but it is so large ($P_m \gg P_{\max}$) that it bears no practical importance. The physical reason for this is that the only way to reduce, at reasonably low pressure (P_m), the large percentage difference between the two lattice constants, is to have comparably large percentage difference between the two elastic moduli; this is contrary to the present requirement. Therefore, the two lattice constants cannot be matched at low values of P_m.

For HJ's the results follow from Sec. III and (25):

$$\varepsilon^{\parallel}(P) = f - \frac{P}{3B_s}(1 + f\ ), \tag{56a}$$

$$\Delta\varepsilon(P) = \Delta\varepsilon\left(1 - \frac{P}{3B_s}\right), \tag{56b}$$

$$\varepsilon^{\perp}(P) = \varepsilon^{\perp} - \frac{P}{3BB_s}\left[B_s + fB(1 - \Delta\tilde{\varepsilon})\right], \tag{56c}$$

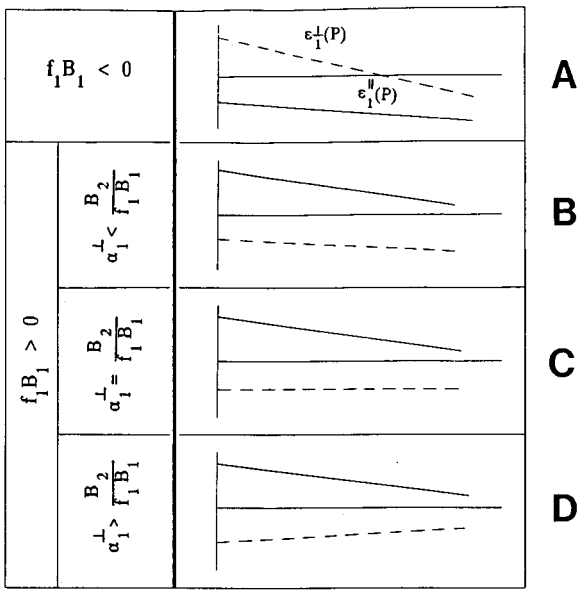

FIG. 5. Same as Fig. 3 under the condition $|f_\nu| \gg |\Delta B/B_\nu|$. For HJ's along [001] the condition imposed by $\alpha_1^{\perp}$ in row B becomes $B^s/fB < 2C_{12}/C_{11}$. Analogous changes apply to rows C and D.

$$\varepsilon_s^{\parallel}(P) = \varepsilon_s^{\perp}(P) = -\frac{P}{3B_s}, \quad \Delta\varepsilon_s(P) = 0, \tag{57}$$

where P_m is given by (54). The compressibilities are as in (45a), (45b), and

$$\kappa^{\perp} = \kappa_s + \kappa\Delta\varepsilon. \tag{58}$$

Before closing this section, the following comment should be made. The strain analysis presented here in cases IV A, IV B, and IV C concerns each of the two layers independently. Thus, in considering the condition $|f_\nu| \ll |\delta\beta/\beta_{\nu'}|$ in Sec. IV A, we have assumed that if $|f_1| \ll |\delta\beta/\beta_2|$, it does not necessarily mean that $|f_2| \ll |\delta\beta/\beta_1|$. However, if we impose the condition that the critical temperatures of both layers be equal, it is easy to show, using (11), that with the exemption of some extreme cases, satisfaction of any of these conditions is independent of ν and ν'. Thus, classifying a combination according to Secs. IV A, IV B, or IV C, requires checking either and only one of the two constituents of the combination. These comments are valid for the P effects as well.

V. APPLICATIONS

We have chosen three combinations of materials to apply the present theoretical results, i.e., ZnSe/GaAs, ZnSe/ZnTe, and ZnSe/GaSb corresponding to the categories of Secs. IV A, IV B, and IV C, respectively.

We start with an undercritical ZnSe epilayer grown along [001] on a GaAs substrate. Since $f \equiv f_1 = -2.7\times10^{-3} < 0$ and $\delta\beta \simeq -2.6\times10^{-6}/\mathrm{K} < 0$ (over the entire range covered by the experimental data $100 \leqslant T \leqslant 500$) the expected linear trends for $\varepsilon^{\parallel}(T)$ and $\varepsilon^{\perp}(T)$ are similar to those in Fig. 1, row A, column $f_1 < 0$. The actual results, based on (31) and (35c) are shown by solid lines in Fig. 6(a). No intersection occurs for any real value of T since $f/\delta\beta \simeq 1000\ \mathrm{K} > T_0 = 300\ \mathrm{K}$ [see

comment (iii) following (33)]. The experimental points in the same figure are taken from Ref. 12 where such data have been obtained by x-ray diffraction techniques for HJ's of ZnSe/GaAs [001] with various thicknesses. The data correspond to the smallest thickness used in Ref. 12, i.e., $h \simeq 0.2$ μm. This value is near the critical thickness $h_c \simeq 0.15$ to 0.20 μm of this particular combination. The values of the various parameters used for the computation are $a = 5.6687$ Å, $a_s = 5.65325$ Å, $\beta = 6.6\times10^{-6}$/K, and $\beta_s = 4\times10^{-6}$/K $(100 \leqslant T \leqslant 500)$, $C_{11} = 81.05\times10^{11}$ GPa, $C_{12} = 48.8\times10^{11}$ GPa, $\Delta\tilde{\varepsilon} = 1 + 2C_{12}/C_{11} = 2.18$, $\varepsilon^{\perp} = (1-\Delta\tilde{\varepsilon})\varepsilon^{\parallel} = 3.2\times10^{-3}$. For completeness we calculate the TEC's of the system at $T_g (= 280\,^{\circ}\text{C})$.[12] From (37) we find $\beta^{\parallel}_{\rm HJ} = \beta^{\perp}_{\rm HJ} = \beta_s = 6.6\times10^{-6}$/K, $\beta^{\perp} = 1.2\times10^{-5}$/K, and $\beta_{\rm HJ} = 2\times10^{-5}$/K.

The agreement between computed and experimental results is satisfactory but can be further improved if the T dependence of β and β_s is taken into account. Data for $\beta(T)$ of ZnSe and GaAs exist in literature in various places. We have used the data from Ref. 13, shown by experimental points in Figs. 7(a) and 7(b), respectively. In order to apply Eq. (4) we need analytical functions for $\beta(T)$ consistent with such data. The solid lines in Figs. 7(a) and 7(b) represent such fitted functions which, we have found, have the following logarithmic forms

$$\beta(T) = (3.43 \ln T - 12.4)\times10^{-6}/\text{K} \quad \text{for ZnSe } 100 \leqslant T \leqslant 500, \tag{59a}$$

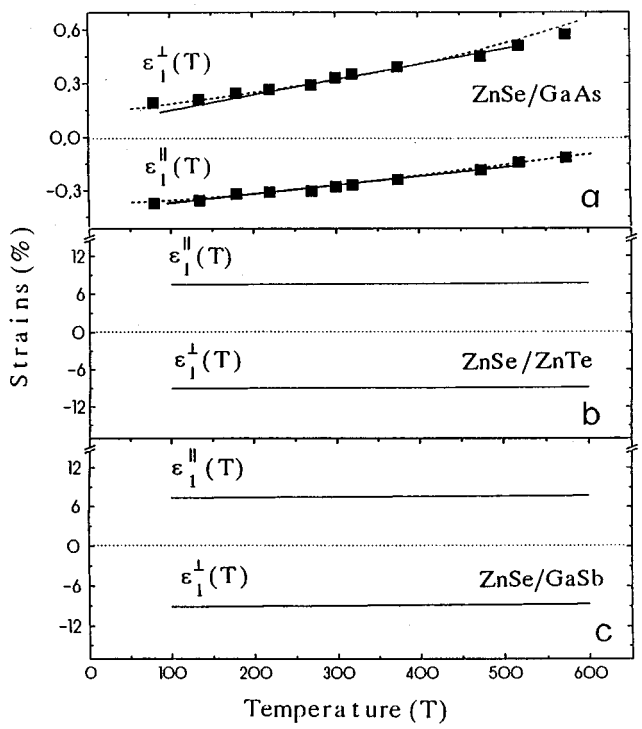

FIG. 6. Computed results based on the present analysis for the three cases described in Sec. V. Solid (dashed) lines correspond to T-independent (T-dependent) thermal expansion coefficients. The data are from Ref. 12.

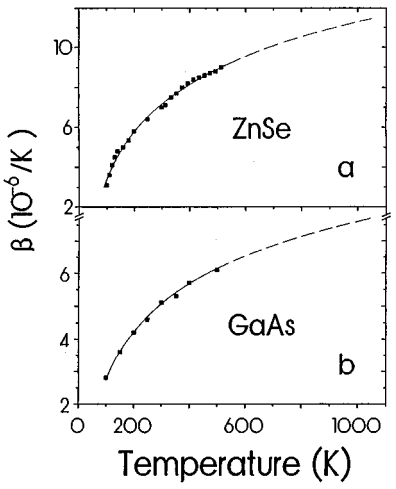

FIG. 7. Experimental points for the function $\beta(T)$ of (a) ZnSe and (b) GaAs taken from Ref. 13. Fitted solid curves obey Eqs. (59a) and (59b). The dashed lines correspond to extrapolations.

$$\beta(T) = (2.1 \ln T - 6.8)\times10^{-6}/\text{K} \quad \text{for GaAs } 100 \leqslant T \leqslant 500. \tag{59b}$$

The dashed portions of the curves correspond to extrapolations not supported by actual data, and should therefore be used with caution.

The final results based on the mean values of β's and Eqs. (35a) and (35c) are shown by dashed lines in Fig. 6(a). The new curves show an improved agreement with the data and indicate the significance of properly handling the T dependence of TEC's. Further improvement can be expected if the T dependence of the elastic constants is also taken into account. The same HJ of ZnSe/GaAs has also been studied experimentally by Cui *et al.*[4] (Raman scattering under pressure). The data are in very good agreement with the results of Sec. IV A and discussed in detail in Ref. 2.

Next we consider the undercritical epilayer of ZnSe on a ZnTe substrate under the same conditions as before. Here $f \equiv f_1 = 7.6\% > 0$ and $\delta\beta + f\beta_s = 1.1\times10^{-6}/\text{K} > 0$; the expected linear trends for $\varepsilon^{\parallel}(T)$ and $\varepsilon^{\perp}(T)$ are similar to those in Fig. 2, row C, column $f_1 > 0$. The actual results, based on (38a) and (38d) are shown by solid lines in Fig. 6(b). We have used $a_s = 6.1$ Å, and the data for $\beta_s(T)$ from Ref. 13, shown by experimental points in Fig. 8(a). The analytical function consistent with such data is shown by the solid line in Fig. 8(a) and is best represented by the polynomial form

$$\beta_s(T) = (\alpha_0 + \alpha_1 T + \alpha_2 T^2 + \alpha_3 T^3 + \alpha_4 T^4 + \alpha_5 T^5)\times10^{-6}/\text{K} \quad (\text{ZnTe},\ 100 \leqslant T \leqslant 300), \tag{60}$$

where $\alpha_0 = -31.212$, $\alpha_1 = 0.7983$, $\alpha_2 = -6.767$, $\alpha_3 = 2.9\times10^{-5}$, $\alpha_4 = -6.193\times10^{-8}$, $\alpha_5 = 0.523\times10^{-10}$. No intersection occurs for any real value of T since $f/(f\beta_s + \delta\beta) \cong 7\times10^4 > T_0$. The strains in this case appear nearly insensitive to the changes of T. We are not aware of any experimental data for T or P effects in this or any other undercritical combination belonging to this case.

Finally we consider an undercritical epilayer of ZnSe on a GaSb substrate under the same conditions as before. Here $f \equiv f_1 = 7.5\% > 0$ and $\alpha^{\perp} = 1.18 < \beta/f\beta_s = 12.5$; the expected

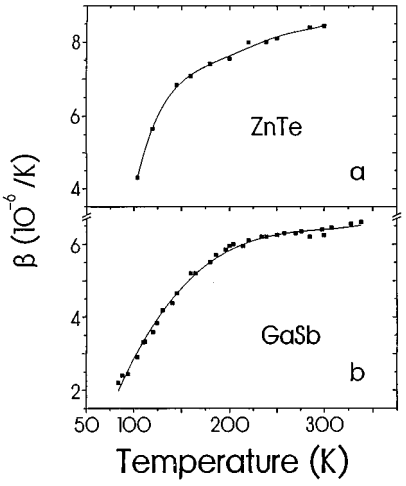

FIG. 8. Experimental points for the function $\beta(T)$ of (a) ZnTe and (b) GaSb taken from Ref. 13. Fitted solid curves obey Eqs. (60) and (61).

linear trends for $\varepsilon^{\parallel}(T)$ and $\varepsilon^{\perp}(T)$ are similar to those in Fig. 4, row B. The actual results, based on (49a) and (49c) are shown by solid lines in Fig. 6(c). We have used $a_s=6.09593$ Å and the data for $\beta_s(T)$ from Ref. 13, shown by experimental points in Fig. 8(b). The analytical function consistent with such data is shown by the solid line in Fig. 8(b) and represented by

$$\beta_s(T)=(\alpha_0+\alpha_1 T+\alpha_2 T^2+\alpha_3 T^3)\times 10^{-6}/\mathrm{K}$$
$$(\mathrm{GbSb},\ \ 100<T<300), \tag{61}$$

where $\alpha_0=-4.98267$, $\alpha_1=0.11039$, $\alpha_2=-3.62459\times 10^{-4}$, $\alpha_3=4.03657\times 10^{-7}$. No intersection occurs for any real value of T since $T_m=-1/\beta_s+T_0<0$. The strains are very insensitive to any changes of T. We are not aware of any experimental data for T or P effects in this or any other undercritical combination belonging to this case.

VI. CONCLUSION

The effects of temperature on strained undercritical SL's and HJ's grown along arbitrary directions have been examined in detail, in the temperature region where no phase transitions take place. The study refers to the temperature dependence of elastic strains, stresses, and the linear thermal expansion coefficients of the material system; it also includes analogous pressure effects on strains, stresses, and linear compressibilities, thus extending previously published work by one of the authors. The elastic constants are treated as temperature independent. As demonstrated with real examples (ZnSe/GaAs, ZnSe/ZnTe, ZnSe/GaSb), it is necessary to handle all thermal expansion coefficients through their average values in the corresponding temperature regions. An important conceptual parameter is the critical temperature T_m, for which the unit cells recover their cubic shapes. Over T_m, the tetragonal distortions reverse signs; the same applies to physical phenomena that depend linearly on the strains, such as piezoelectric fields in III-V or II-VI constituents.[10] The critical temperature may be lower or higher than room temperature. It may also be negative; in the latter case the tetragonal distortions never reverse their signs. Specific examples have been treated in detail. For ZnSe/GaAs [001] the present computed results and the experimental data from the literature are in good agreement. The strains in the case of ZnSe/GaAs show substantial variation with temperature, contrary to the situations of ZnSe/ZnTe and ZnSe/GaSb where the variations are negligible.

Raman spectroscopy is certainly a very direct technique for observing T- and P-tuned strains in SL's and HJ's, as demonstrated by the results of Cui *et al.* (Ref. 4). Other techniques are equally appropriate in this regard, e.g., photoluminescence,[14–17] photoreflectance,[3,18] piezo- and electroreflectance.[3] In these situations the effects of T and P on strains become evident through the corresponding changes in the electronic structure of such systems.

The present work and the work in EA address the problem of undercritical structures only. The situation in overcritical systems is expected to be more involved since the strains are of mixed character (lattice and thermal misfit), they depend on thickness, and they are not homogeneous within each layer. Similar effects due to temperature and pressure variations are expected to occur and have, in fact, been observed in numerous cases of overcritical systems. No systematic theoretical treatment of such effects has been presented so far, to our knowledge. An analogous treatment of these problems will be the subject of a future work.

ACKNOWLEDGMENTS

Partial support by the General Secretariat for Research and Technology, Greece. One of us (T.D.W.) is grateful to the Greek Ministry of National Economy for a scholarship.

APPENDIX

The general results of this appendix have been described in detail elsewhere[7–9] and refer to fixed temperature T_0. Wherever obvious, the layer index $\nu=1,2$ is omitted for simplicity. We set $\varepsilon_3'\equiv\varepsilon^{\perp}$ (strain normal to the plane) and $\varepsilon_1'=\varepsilon_2'\equiv\varepsilon^{\parallel}$ (in-plane isotropic strains discussed in the text).

The reduced tetragonal distortion of the layer $\Delta\tilde{\varepsilon}$ is computed directly from l_3, m_3, n_3 and the layer's stiffnesses C_{ij},

$$\Delta\tilde{\varepsilon}\equiv\Delta\varepsilon/\varepsilon^{\parallel}=(\varepsilon^{\parallel}-\varepsilon^{\perp})/\varepsilon^{\parallel}$$
$$=\frac{3B}{\Delta}\,[C_{44}^2+CC_{44}(1-T_{33})+3C^2(l_3m_3n_3)^2], \tag{A1}$$

where $B=(C_{11}+2C_{12})/3$ is the bulk modulus, and

$$C=C_{11}-C_{12}-2C_{44}, \tag{A2a}$$

$$T_{ij}=T_{ji}=T_{\lambda\mu\kappa\rho}=l_\lambda l_\mu l_\kappa l_\rho+m_\lambda m_\mu m_\kappa m_\rho+n_\lambda n_\mu n_\kappa n_\rho, \tag{A2b}$$

$$\Delta=C_{11}C_{44}^2+(CC_{44}/2)(C_{11}+C_{12})(1-T_{33})$$
$$+C^2(C_{11}+2C_{12}+C_{44})(l_3m_3n_3)^2. \tag{A2c}$$

Roman (Greek) indices run from 1(1) to 6(3). The shear elastic modulus G_ν of the νth layer is determined from the corresponding $\Delta\tilde{\varepsilon}_\nu$

$$G_\nu = 3B_\nu(3-\Delta\tilde{\varepsilon}_\nu). \tag{A3}$$

G_ν is used for the evaluation of $a^{\parallel}$, $\varepsilon_\nu^{\parallel}$, and $\beta_{\mathrm{SL}}^{\parallel}$ through Eqs. (6), (7), and (19), respectively. The nonzero strain-stress components, in terms of $\varepsilon^{\parallel}$, are

$$\varepsilon^{\perp} = (1-\Delta\tilde{\varepsilon})\varepsilon^{\parallel}, \tag{A4}$$

$$2\varepsilon'_{23} = \varepsilon'_4 = \frac{3BC}{\Delta}\,[C_{44}T_{34} + C(T_{31}T_{34} - T_{35}T_{36})]\varepsilon^{\parallel}, \tag{A5a}$$

$$2\varepsilon'_{31} = \varepsilon'_5 = \frac{3BC}{\Delta}\,[C_{44}T_{35} + C(T_{32}T_{35} - T_{36}T_{34})]\varepsilon^{\parallel}, \tag{A5b}$$

$$\sigma'_1 = 3B\varepsilon^{\parallel} - (C_{12} + CT_{31})\Delta\varepsilon + C(T_{14}\varepsilon'_4 + T_{15}\varepsilon'_5) \tag{A6a}$$

$$\sigma'_2 = 3B\varepsilon^{\parallel} - (C_{12} + CT_{32})\Delta\varepsilon + C(T_{24}\varepsilon'_4 + T_{25}\varepsilon'_5) \tag{A6b}$$

$$\sigma'_6 = -CT_{36}\Delta\varepsilon + C(T_{25}\varepsilon'_4 + T_{14}\varepsilon'_5). \tag{A6c}$$

All expressions given in this appendix can be used also for HJ with $h_1 \ll h_2$.

[1] Judah A. Tuchman and Irving P. Herman, Phys. Rev. B **45**, 11 929 (1992).

[2] E. Anastassakis, Phys. Rev. B **46**, 13 244 (1992).

[3] R. J. Thomas, M. S. Boley, H. R. Chandrasekhar, M. Chandrasekhar, C. Parks, A. K. Ramdas, J. Han, M. Kobayashi, and R. L. Gunshor, Phys. Rev. B **49**, 2181 (1994).

[4] S. M. Hu, J. Appl. Phys. **69**, 7901 (1991); **70**, R53 (1991), and references therein; L. J. Cui, U. D. Venkateswaran, B. A. Weinstein, and B. T. Jonker, Phys. Rev. B **44**, 10 949 (1991).

[5] D. J. Olego, K. Shahzad, J. Petruzzello, and D. Cammack, Phys. Rev. B **36**, 7674 (1987).

[6] F. Anastassakis and E. Liarokapis, Phys. Status Solidi (b) **149**, K1 (1988).

[7] E. Anastassakis, J. Appl. Phys. **68**, 4561 (1990).

[8] E. Anastassakis, J. Cryst. Growth **114**, 647 (1991).

[9] E. Anastassakis, Solid State Commun. **78**, 347 (1991).

[10] E. Anastassakis, Phys. Rev. B **46**, 4744 (1992).

[11] J. F. Nye, *Physical Properties of Crystals* (Oxford University Press, New York, 1964).

[12] T. Matsumoto, T. Iijima, and T. Ishida, Jpn. J. Appl. Phys. **27**, 892 (1988).

[13] *Semiconductors. Physics of Group IV Elements and III-V Compounds*, edited by K.-H. Hellwege and O. Madelung, Landolt-Börnstein, New Series, Group III, Vol. 17, Pt. a (Springer, New York, 1982); *Physics of II-VI and I-VII Compounds, Semimagnetic Semiconductors*, edited by O. Madelung and M. Schulz, Landolt-Börnstein, New Series, Group III, Vol. 17, Pt. b (Springer, New York, 1982).

[14] M. Gerling, M.-E. Pistol, L. Samuelson, W. Seifert, J.-O. Fornell, and L. Ledebo, Appl. Phys. Lett. **59**, 806 (1991).

[15] M. Holtz, R. Cingolani, K. Reimann, R. Muralidharan, K. Syassen, and K. Ploog, Phys. Rev. B **41**, 3641 (1990).

[16] Y. Yamada, Y. Masumoto, T. Taguchi, and K. Takemura, Phys. Rev. B **44**, 1801 (1991).

[17] J. A. Tuchman, S. Kim, Z. Sui, and I. P. Herman, Phys. Rev. B **46**, 13 371 (1992).

[18] B. Rockwell, H. R. Chandrasekhar, M. Chandrasekhur, A. K. Ramdas, M. Kobayashi, and R. L. Gunshor, Phys. Rev. B **44**, 11 307 (1991).